



# Synthesis of liquid crystalline anthraquinolyl–triphenylenes

Graeme Cooke,<sup>a,\*</sup> Neetu Kaushal,<sup>b</sup> Neville Boden,<sup>c</sup> Richard J. Bushby,<sup>c</sup> Zhibao Lu<sup>c</sup> and Owen Lozman<sup>c</sup>

<sup>a</sup>*Department of Chemistry, Heriot-Watt University, Riccarton, Edinburgh EH14 4AS, UK*

<sup>b</sup>*School of Applied and Molecular Sciences, University of Northumbria at Newcastle, Ellison Building, Newcastle upon Tyne NE1 8ST, UK*

<sup>c</sup>*School of Chemistry and SOMS Centre, University of Leeds, Leeds LS2 9JT, UK*

Received 3 July 2000; accepted 10 August 2000

---

## Abstract

The synthesis, electrochemistry and mesogenic properties of novel anthraquinolyl–triphenylenes are described. <sup>1</sup>H NMR, UV–vis, solution electrochemistry and molecular modelling studies indicate that an intermolecular charge–transfer interaction occurs between the anthraquinone moiety and the triphenylene nucleus. © 2000 Elsevier Science Ltd. All rights reserved.

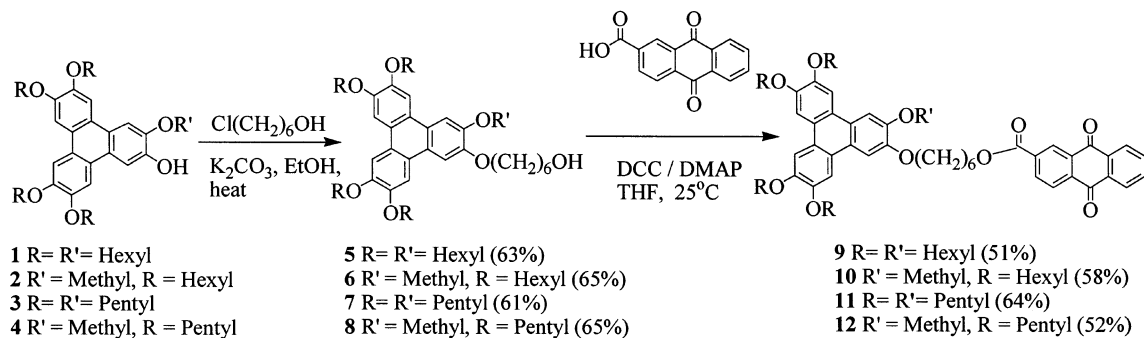
---

The study of discotic liquid crystals bearing pendant planar, electron deficient units is a burgeoning field.<sup>1</sup> A number of discotic cores have been utilised in these studies, however, in all of the reported examples the electron deficient moiety has been limited to the trinitrofluorenone unit. In the present work, we report the synthesis and properties of the first examples of anthraquinolyl–hexaalkyloxytriphenylenes. Supramolecular formulations of this type are particularly exciting as the ionisation potential of the triphenylene unit and the electron affinity of the anthraquinone unit are well matched, and should readily give rise to inter- and intramolecular charge–transfer (C–T) complexes with novel redox controllable supramolecular architectures<sup>2</sup> with rectification and electron transfer applications.<sup>3</sup> The stability of the columnar phases formed in such systems is also of considerable current interest. Initially it was believed that the C–T interaction was itself the cause, but much of the earlier work has been successfully interpreted in terms of quadrupolar<sup>4</sup> or CPI<sup>5</sup> interactions.

The triphenylene building blocks **5–8** were prepared from alcohols **1–4**<sup>6</sup> by a K<sub>2</sub>CO<sub>3</sub> catalysed Williamson's reaction with 6-chlorohexan-1-ol.<sup>7</sup> Triphenylenes **9–12** were then prepared in good yield by a DCC/DMAP catalysed esterification with anthraquinone-2-carboxylic acid in THF at 25°C (Scheme 1).

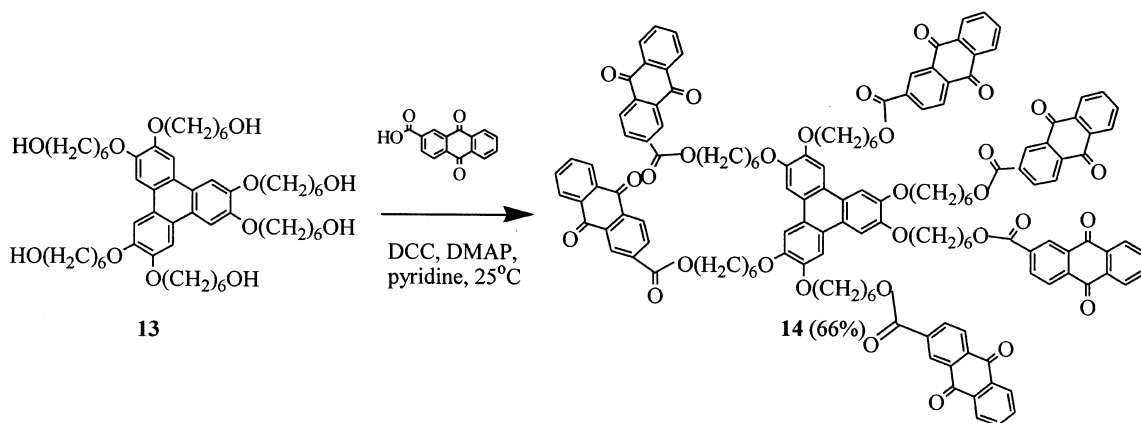
---

\* Corresponding author. Fax: 0131 451 3180; e-mail: G.Cooke@hw.ac.uk



Scheme 1.

Here, we also describe the synthesis of new prototype structures in which we have a triphenylene nucleus bearing six anthraquinone units. Hexa-hexylhydroxytriphenylene **13**<sup>7</sup> was reacted with excess anthraquinone-2-carboxylic acid to afford **14** in good yield (Scheme 2).



Scheme 2.

We have investigated the solution electrochemistry of these compounds using cyclic voltammetry (CV). The half wave potentials are presented in Table 1. The triphenylene precursors **5–8** and **13** all displayed two reversible oxidations at +1.07 and +1.28 V due to the formation of the radical cation and dicationic species, respectively.<sup>8</sup> The anthraquinonyl–triphenylenes **9–12** each gave rise to two reduction waves corresponding to the reversible formation of the anthraquinonyl radical anion and the irreversible formation of the dianion species. Two oxidation waves were also observed for these species due to the formation of the triphenylene radical cation and dicationic species, respectively. The voltammogram of derivative **14** displays a single oxidation peak at +1.08 V for the triphenylene core, together with reduction peaks at –0.70 and –1.29 V, due to the reversible formation of the radical anionic states and irreversible formation of the dianionic states of all six anthraquinone moieties. For derivatives **9–12** and **14**, a 30 mV decrease in the oxidation potentials of the triphenylene unit is observed compared to that of the non-anthraquinone containing precursors. Furthermore, the reduction potentials of the anthraquinone moiety of these derivatives are also shifted by 70 mV to higher reduction potentials compared to that of 2-ethoxycarbonylanthraquinone **15**. The data are indicative of

C–T interactions between the electron rich triphenylene unit and the electron deficient anthraquinone unit.

Table 1  
Cyclic voltammetry data<sup>a</sup>

Compound	$E_{1/2}^1$	$E_{1/2}^2$	$E_{1/2}^3$	$E_{1/2}^4$
<b>5</b>	+1.28	+1.07		
<b>9</b>	+1.25	+1.04	−0.70	−1.29
<b>10</b>	+1.25	+1.04	−0.70	−1.29
<b>11</b>	+1.25	+1.04	−0.70	−1.29
<b>12</b>	+1.25	+1.04	−0.70	−1.29
<b>14</b>		+1.04	−0.77	−1.31
<b>15</b>			−0.76	−1.25

<sup>a</sup> In volts, 0.5 M TBA ClO<sub>4</sub>/CH<sub>2</sub>Cl<sub>2</sub> versus Ag/AgCl, scan rate 100 mV s<sup>−1</sup>. Working and counter electrodes: Pt.

We have modelled molecule **10** using the MM+ forcefield,<sup>9</sup> which produced the two low energy structures provided in Fig. 1a and b. Clearly, the less exothermic heat of formation of the structure represented in Fig. 1b, compared to Fig. 1a, argues against intramolecular C–T interactions occurring. This is probably due to the lack of conformational flexibility of the hexyl-chain connecting the anthraquinone to the triphenylene nucleus. The modelling data supports our extensive UV–vis experimental studies performed on derivatives **9–12** and **14**, which have shown that the electron rich and electron deficient units have the propensity of forming intermolecular C–T interactions by displaying an absorption band centred at 490 nm at concentrations greater than 10<sup>−4</sup> M. Furthermore, the addition of one equivalent of **15** to a solution of **5** in CHCl<sub>3</sub> results in the formation of a red solution, which confirms that C–T interactions can occur intermolecularly.

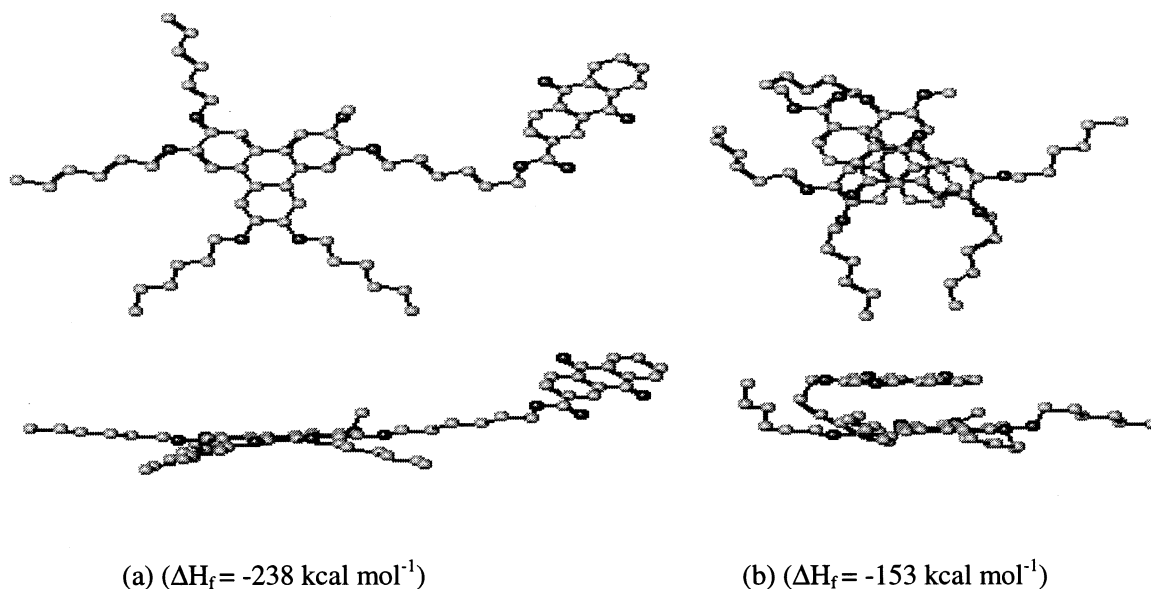


Figure 1. MM+ Energy minimised structures of **10**. Hydrogens have been removed for clarity

We have investigated the mesogenic properties of the new compounds using polarising optical microscopy and differential scanning calorimetry. The results are summarised in Table 2. In all cases the triphenylene precursors **5–8** and **13** did not display a discotic mesophase. Derivative **10** showed two peaks in the first DSC run corresponding to melting and clearing transitions. On cooling, the liquid supercooled and remained isotropic well below room temperature. A spherulite texture was observed through cross polarising filters after 24 hours at room temperature, and is typical of a hexagonal phase. Derivative **12** was also observed to supercool in this way, however, no mesophase was observed. For the derivative **10**, it is tempting to speculate that the formation of the columnar mesophase is promoted by a combination of the correct peripheral alkyl chain length and the presence of a methoxy-unit attached to the benzeneoid unit bearing the anthraquinone unit which provides a spacer group to accommodate this relatively bulky moiety in the mesophase architecture. Derivatives **9** and **11**, without this seemingly important spacer group, displayed only K–I transitions when examined using DSC and polarising optical microscopy. Compound **14** bearing six anthraquinone units failed to display a mesophase.

Table 2  
Transition temperatures and thermodynamic ( $\Delta H$ ,  $\text{kJ mol}^{-1}$ ) data for mesophase transitions observed for **9–12** and **14** as determined by DSC (sealed aluminium pans)<sup>a</sup>

Compound	K–K1 (°C)	K1–Col (°C)	Col–I (°C)	K1–K2 (°C)	K–I (°C)
<b>9</b>					53–57 (–31.4)
<b>10</b>	59 (–7.7)	89 (–6.2)	102°C (–47.4)		
<b>11</b>					52–55 (–30.2)
<b>12</b>	33 (–1.9)			66 (–1.6)	113 (–0.5)
<b>14</b>	70 (–12.2)			98 (–27.3)	

<sup>a</sup> Heating rate  $10^\circ\text{C min}^{-1}$ .

In conclusion, we have synthesised the first example of a liquid crystalline anthraquinolytriphenylene. <sup>1</sup>H NMR, CV, UV–vis and modelling studies have indicated that an intermolecular C–T interaction takes place between the electron rich triphenylene nucleus and the pendant electron deficient anthraquinone moieties.

## Acknowledgements

The author thanks The Royal Society of Chemistry and the Royal Society for financial support and the EPSRC National Mass Spectrometry Service Centre, Swansea for performing FAB mass spectral analysis.

## References

- (a) Bengs, H.; Ebert, M.; Karthaus, O.; Kohne, B.; Praefcke, K.; Ringsdorf, H.; Wendorff, J. H.; Wustefeld, R. *Adv. Mater.* **1990**, *2*, 41; (b) Markovitsi, D.; Bengs, H.; Pfeffer, N.; Charra, F.; Nunzi, J.-M. *J. Chem. Soc. Faraday Trans.* **1992**, *88*, 1275–1279; (c) Janietz, D. *Chem. Commun.* **1996**, 713–714; (d) Mahlstedt, S.; Janietz, D.; Schmidt, C.; Stracke, A.; Wendorff, J. H. *Liq. Cryst.* **1999**, *26*, 1359–1369; (e) Mahlstedt, S.; Janietz, D.; Schmidt, C.; Stracke, A.; Wendorff, J. H. *Chem. Commun.* **2000**, 15–16.

2. Boulas, P. L.; Gomez-Kaifer, M.; Echegoyen, L. *Angew. Chem., Int. Ed.* **1998**, *37*, 216–247.
3. Metzger, R. M. *J. Mater. Chem.* **1999**, *9*, 2027–2036.
4. Bates, M. A.; Luckhurst, G. R. *Liq. Cryst.* **1998**, *24*, 229.
5. Arikainen, E. O.; Boden, N.; Bushby, R. J.; Lozman, O. R.; Wood, A.; Vinter, J. G. *Angew. Chem., Int. Ed.* **2000**, *39*, 2333–2336.
6. (a) Cooke, G.; Hell, F.; Violini, S. *Synth. Commun.* **1997**, *27*, 3745–3748; (b) Boden, N.; Bushby, R. J.; Cammidge, A. N.; Martin, P. S. *J. Mater. Chem.* **1995**, *5*, 1857–1860.
7. Cooke, G.; Radhi, A.; Boden, N.; Bushby, R. J.; Brown, S.; Heath, S. L. *Tetrahedron* **2000**, *56*, 3385–3390.
8. Bechgaard, K.; Parker, V. D. *J. Am. Chem. Soc.* **1972**, *94*, 4749–4750.
9. As implemented in HyperChem 5.1, Hypercube Inc., Gainesville, FL. Initial geometries were obtained using the MM+ forcefield. Single point calculations using PM3 semi-empirical procedures were then used to calculate the Mulliken charges on the atoms. The geometries of these systems were then re-optimised using the MM+ forcefield to yield the structures provided in this manuscript. The heat of formation of these molecules were then calculated using a further PM3 single point calculation.